



**University of
Zurich**^{UZH}

**Zurich Open Repository and
Archive**

University of Zurich
University Library
Strickhofstrasse 39
CH-8057 Zurich
www.zora.uzh.ch

Year: 2013

Ultraclean freestanding graphene by platinum-metal catalysis

Longchamp, Jean-Nicolas ; Escher, Conrad ; Fink, Hans-Werner

DOI: <https://doi.org/10.1116/1.4793746>

Posted at the Zurich Open Repository and Archive, University of Zurich

ZORA URL: <https://doi.org/10.5167/uzh-93614>

Journal Article

Published Version

Originally published at:

Longchamp, Jean-Nicolas; Escher, Conrad; Fink, Hans-Werner (2013). Ultraclean freestanding graphene by platinum-metal catalysis. *Journal of Vacuum Science Technology B*, 31(2):020605.

DOI: <https://doi.org/10.1116/1.4793746>

Ultraclean freestanding graphene by platinum-metal catalysis

Jean-Nicolas Longchamp, Conrad Escher, and Hans-Werner Fink

Citation: *Journal of Vacuum Science & Technology B* **31**, 020605 (2013); doi: 10.1116/1.4793746

View online: <http://dx.doi.org/10.1116/1.4793746>

View Table of Contents: <http://scitation.aip.org/content/avs/journal/jvstb/31/2?ver=pdfcov>

Published by the AVS: Science & Technology of Materials, Interfaces, and Processing

Articles you may be interested in

N-doped graphene-supported Pt and Pt-Ru nanoparticles with high electrocatalytic activity for methanol oxidation
J. Renewable Sustainable Energy **5**, 021405 (2013); 10.1063/1.4798433

MnO₂ nanotube-Pt/graphene mixture as an ORR catalyst for proton exchange membrane fuel cell
AIP Conf. Proc. **1512**, 370 (2013); 10.1063/1.4791065




Low-energy electron transmission imaging of clusters on free-standing graphene
Appl. Phys. Lett. **101**, 113117 (2012); 10.1063/1.4752717

Greatly enhanced adsorption and catalytic activity of Au and Pt clusters on defective graphene
J. Chem. Phys. **132**, 194704 (2010); 10.1063/1.3427246

Metal-catalyzed crystallization of amorphous carbon to graphene
Appl. Phys. Lett. **96**, 063110 (2010); 10.1063/1.3318263



Instruments for Advanced Science

<p>Contact Hiden Analytical for further details: W www.HidenAnalytical.com E info@hiden.co.uk CLICK TO VIEW our product catalogue</p>	 <p>Gas Analysis</p> <ul style="list-style-type: none"> › dynamic measurement of reaction gas streams › catalysis and thermal analysis › molecular beam studies › dissolved species probes › fermentation, environmental and ecological studies 	 <p>Surface Science</p> <ul style="list-style-type: none"> › UHV TPD › SIMS › end point detection in ion beam etch › elemental imaging - surface mapping 	 <p>Plasma Diagnostics</p> <ul style="list-style-type: none"> › plasma source characterization › etch and deposition process reaction › kinetic studies › analysis of neutral and radical species 	 <p>Vacuum Analysis</p> <ul style="list-style-type: none"> › partial pressure measurement and control of process gases › reactive sputter process control › vacuum diagnostics › vacuum coating process monitoring
--	--	--	--	--

Ultraclean freestanding graphene by platinum-metal catalysis

Jean-Nicolas Longchamp,^{a)} Conrad Escher, and Hans-Werner Fink
Physics Institute, University of Zurich, Winterthurerstrasse 190, 8057 Zurich, Switzerland

(Received 18 January 2013; accepted 15 February 2013; published 1 March 2013)

While freestanding clean graphene is essential for various applications, existing technologies for removing the polymer layer after transfer of graphene to the desired substrate still leave significant contaminations behind. The authors discovered a method for preparing ultraclean freestanding graphene utilizing the catalytic properties of platinum metals. Complete catalytic removal of polymer residues requires annealing in air at a temperature between 175 and 350 °C. Low-energy electron holography investigations prove that this method results in ultraclean freestanding graphene. © 2013 American Vacuum Society. [<http://dx.doi.org/10.1116/1.4793746>]

I. INTRODUCTION

The physical and electronic properties of graphene^{1,2} depend to a large extent on its defect-free structure and its cleanliness. Scattering of transport electrons at impurities is one of the major drawbacks in the use of graphene in electronic devices.^{3–5} When employing graphene as a substrate in electron microscopy, the presence of residues is frustrating because these features are often of the same size as the object under study.⁶ While the growth of defect-free single-layer graphene by means of chemical vapor deposition (CVD) is nowadays routinely possible,^{7,8} easily accessible and reliable techniques to transfer graphene to different substrates in a clean manner are still lacking. The common technique for the transfer of the layers grown by means of CVD on a metallic substrate (usually nickel or copper) onto an arbitrary substrate is based on the use of a polymer layer, ordinarily polymethyl methacrylate (PMMA), spread or spin-coated over graphene.^{4,9,10} The removal of the approximately 100 nm thick PMMA layer is a challenge and extensive efforts have been undertaken in the past few years to establish a reliable technique to retrieve the pristine graphene without PMMA residues.^{3–5,11–14} Well-known chemical etchants for PMMA are acetone and chloroform.¹⁵ Unfortunately, wet chemical treatment of the polymer leads to contaminated graphene layers with lots of residues left behind. Thermal annealing at temperature in the range of 300–400 °C in vacuum^{14,15} or in an Ar/H₂ atmosphere¹⁵ appears to help the cleaning process. However, besides the fact that these techniques are not easily available, they do not lead to ultraclean freestanding graphene free from hydrocarbon contaminations^{16–18} or polymer residues.^{15,19}

We present here a simple method for preparing ultraclean freestanding graphene based on the removal of a polymer layer by the catalytic activity of the platinum metals Pt and Pd. The cleanliness of the prepared freestanding graphene layers is investigated by means of low-energy electron holography.^{20,21} Electrons with kinetic energies in the range of 50–100 eV are extremely sensitive to the smallest amounts of contamination causing electrical field disturbances originating, for instance, from electrical nonconductive PMMA residues. Furthermore, low-energy electrons exhibit a

scattering cross-section for atoms almost independent of their Z number, an advantage in comparison to TEM in view of detecting the presence of possible hydrocarbon residues.

II. METHODS

All the graphene layers used in this study were grown by the conventional CVD method²² on a polycrystalline copper substrate. A PMMA capping (about 100 nm thick) is subsequently spin-coated onto the graphene [Fig. 1(i)]. The preparation of the clean freestanding graphene starts with the chemical wet-etching of the metallic substrate, as illustrated in Fig. 1(ii). After the complete removal of the underlying copper, the remaining graphene–PMMA complex is rinsed four times with ultrapurified water to wash off the etching solution [Fig. 1(iii)]. The third step of the preparation method consists of the placement of the graphene–PMMA composite on a metal (Pt, Pd)-coated 50 nm thick silicon nitride membrane previously perforated by means of a focused gallium ion beam [Fig. 1(iv)]. After drying, the sample is placed onto a conventional laboratory heating plate for thermal annealing in air at a temperature in the range of 175–350 °C [Fig. 1(v)], i.e., well below the oxidation temperature of graphene in air.^{14,23}

III. RESULTS AND DISCUSSION

Figure 2 illustrates the degradation of the PMMA capping due to the presence of the catalytic metal while it remains present on a noble metal, i.e., gold in this case. On a 10 × 10 mm² microscopy glass plate, about half of its surface is coated with gold and the other half with platinum. A 2 mm gap of uncoated SiO₂ between the two metal layers was arranged in order to avoid cross-diffusion of the metals. Figure 2(a) displays the situation after the transfer of a graphene–PMMA composite onto the glass plate and across the

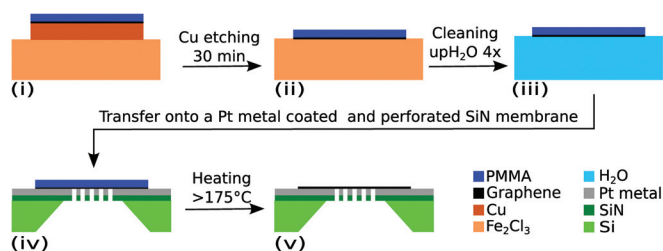


FIG. 1. (Color) Flow chart of the preparation of ultraclean freestanding graphene.

^{a)}Electronic mail: longchamp@physik.uzh.ch

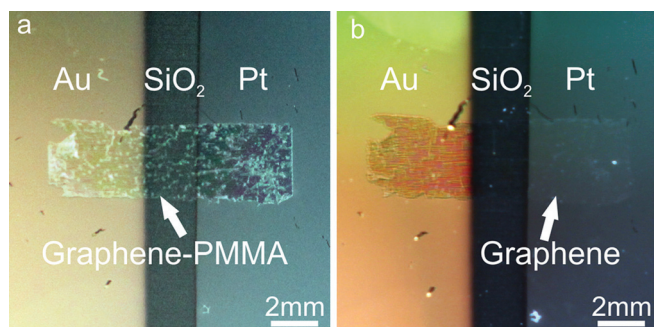


FIG. 2. (Color) (a) Optical photograph of a graphene-PMMA composite transferred onto a glass plate covered with gold and platinum before thermal annealing. (b) Optical photograph of the same sample after thermal annealing at 300 °C for 30 min.

gap between the gold and the platinum layers prior to thermal annealing. The PMMA is clearly visible on both metals. Figure 2(b) shows the result after the annealing of the glass plate at 300 °C for 30 min. The PMMA was decomposed above the platinum layer, leaving clean graphene on the catalytic active metal. Similar results have been obtained for annealing at temperatures in the range of 175–350 °C, provided that the annealing time is properly adjusted. It varies between 6 h for a temperature of 175 °C and just 3 min at 350 °C. As evident from Fig. 2, the PMMA remains present on the gold surface and is apparently undegraded.

Figure 3 shows a light optical microscopy image of the sample presented in Fig. 2, but at higher magnification. As mentioned above, after annealing the PMMA is degraded on the Pt surface while it remains intact on almost the entire SiO₂ surface; a characteristic interference contrast originating from the presence of PMMA on the glass is clearly visible. It is important to note that a several tens of micrometers wide ribbon, along the Pt-metal edge, was also cleaned by the thermal annealing process, leaving bare SiO₂ behind. Apparently, the proximity of platinum is already sufficient to cause a catalytic reaction leading to the decomposition of PMMA. These findings clearly justify the hope that an extended region of clean freestanding graphene can be

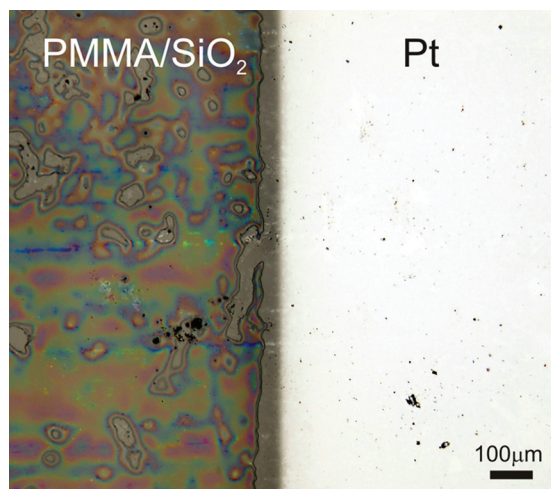


FIG. 3. (Color) Light optical microscopy image of the sample shown in Fig. 2(b).

obtained by the method described above. The supplementary material, movies 1 and 2, shows the degradation of PMMA layers spin-coated onto a SiN chip covered with Pd and Pd-Au, respectively.²⁴ While the PMMA is removed where the Pd is present, it remains on the surface covered with Au (Supplementary material, movie 2).

The thermal degradation of polymers is a complicated process and subject of an entire research field.^{25–27} Various decomposition mechanisms have been proposed, such as random-chain scission, end-chain initiation, unzipping, depropagation or depolymerization, to name just a few. For PMMA in particular, the end-chain initiation has been established as the predominant process.²⁵ A common aspect in all the different decomposition paths is the involvement of hydrogen in the process. Normally, during the thermal degradation of polymers, hydrogen originates from either the backbone or the side chains of the macromolecule, resulting in the formation of smaller molecules or the degradation into monomers. However, this process requires high temperatures, at least 400 °C for PMMA.²⁵ If the molecules produced in this process are small enough, they can escape into the gas phase. In the case presented here, the catalytic aspect of the process can be explained as hydrogenation of the PMMA promoted by the platinum metals such that the cracking of the polymer occurs already at much lower temperatures. The platinum metals are well known in catalysis. It is conceivable that the reaction is initiated by the ability of the Pt-metal to dissociate molecular adsorbed H₂ into atomic hydrogen. The facts that a minimal temperature must be attained to start such a reaction (175 °C in our case), that the time for completing the reaction decreases rapidly with increasing temperature, and that with other metals such as gold the reaction does not proceed at all, are additional strong indications for the catalytic character of the process described here.

In order to investigate the cleanliness of such graphene samples on the nanometer-scale, we prepared freestanding graphene layers placed over holes between 250 and 1000 nm in diameter milled by a focused gallium ion beam into a Pt-coated SiN membrane. In Fig. 4(a), a SEM image of such a hole and in (b) a high magnification image of the substrate surface after sputter deposition of Pt are displayed. The thickness of the platinum layer amounts to 15 nm. It is evident that the metal layer is not uniform but exhibits islands of about 50 nm in size. It is believed that these nanometer-sized domains promote the catalytic activity of the platinum

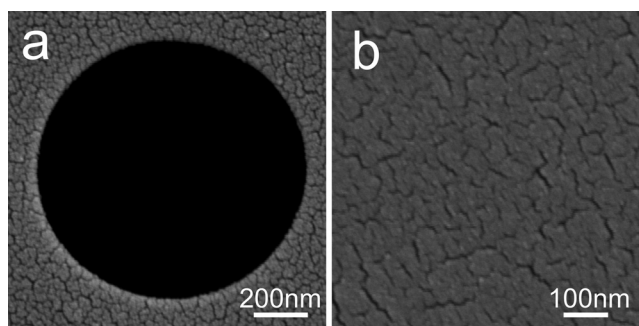


FIG. 4. (a) Scanning electron image of a hole of 1000 nm in diameter milled in a SiN membrane and subsequently coated with Pt. (b) Higher magnification image of the clustered Pt layer.

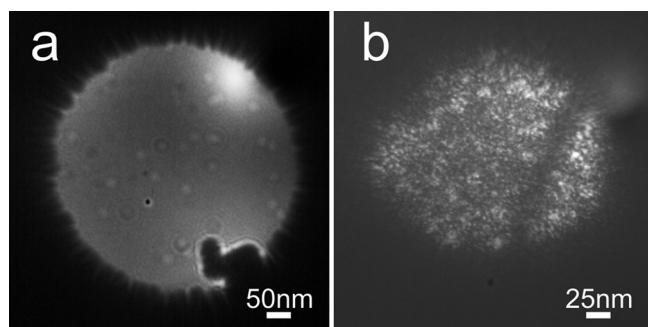


FIG. 5. (a) Low-energy electron hologram of ultraclean freestanding graphene prepared by the method presented here. (b) Electron transmission after the removal of the PMMA layer with acetone.

layer. This is confirmed by the use of smoother Pt layers obtained by e-beam evaporation which leads to an increase of the catalytic reaction time to 45 min at 300 °C in contrast to just 5 min in case of rough sputtered layers.

After the thermal annealing process, the prepared samples were directly transferred to our low-energy electron point source microscope. In this holographic setup inspired by the original idea of Gabor²⁸ of in-line holography, a sharp (111)-oriented tungsten tip acts as source of a divergent beam of highly coherent electrons.²⁹ The electron emitter can be brought as close as 200 nm to the sample with the help of a three-axis piezomanipulator. Part of the electron wave impinging onto the sample is elastically scattered and represents the object wave, while the unscattered part of the wave represents the reference wave.²⁰ At a distant detector, the interference pattern between the object wave and the reference wave—the hologram—is recorded. The magnification in the image is given by the ratio of detector-tip-distance to sample-tip-distance and can be as high as 1×10^6 . Figure 5(a) displays an image of a freestanding ultraclean graphene layer covering a 500 nm diameter hole recorded with our low-energy electron point source microscope at an electron kinetic energy of 61 eV and a total electron current of 50 nA. Apparently, freestanding clean graphene is almost transparent even for low-energy electrons.^{19,30} The presence of graphene can only be confirmed by observing individual adsorbates, possibly from the gas phase, sticking to the monolayer. For comparison, Fig. 5(b) shows an image of freestanding graphene (70 eV, 500 nA), where the polymer layer was removed in the common manner by dissolving it in acetone. The resulting graphene layer is still polluted and almost opaque, even with a tenfold increased electron current, and the presence of PMMA residues is evident.

Similar results as those presented in Fig. 5(a) were also obtained with Pd as catalyst. Attempts to use other metals such as gold for the transfer and cleaning of graphene failed. Low-energy electron microscopy investigations revealed, in these cases, either empty holes where the graphene broke or opaque holes where the graphene was heavily contaminated.

IV. CONCLUSION

In summary, we have demonstrated that the use of platinum metals for the transfer of graphene leads to ultraclean

freestanding layers. The decomposition process of the PMMA layer is of catalytic nature and is promoted by the presence of a platinum metal. Even in the vicinity of the metal the polymer layer is removed, revealing clean graphene on an arbitrary substrate or even freestanding. The degradation reaction proceeds in air and at temperatures ranging from 175 to 350 °C. This preparation method is thus easily accessible in every laboratory and does not require any special equipment. With this, ultraclean graphene is now routinely available to serve not just as substrate for electron microscopy but also in several applications needing ultraclean graphene as prerequisite, such as novel mechanical or electronic mesoscopic devices or as molecular sieves.

ACKNOWLEDGMENT

The authors are grateful for the financial support by the Swiss National Science Foundation.

- ¹K. S. Novoselov, D. Jiang, F. Schedin, T. J. Booth, V. V. Khotkevich, S. V. Morozov, and A. K. Geim, *Proc. Natl. Acad. Sci. U.S.A.* **102**, 10451 (2005).
- ²A. K. Geim and K. S. Novoselov, *Nature Mater.* **6**, 183 (2007).
- ³M. Ishigami, J. H. Chen, W. G. Cullen, M. S. Fuhrer, and E. D. Williams, *Nano Lett.* **7**, 1643 (2007).
- ⁴A. Reina, H. Son, L. Jiao, B. Fan, M. S. Dresselhaus, Z. Liu, and J. Kong, *J. Phys. Chem. C* **112**, 17741 (2008).
- ⁵Y. Dan, Y. Lu, N. J. Kybert, Z. Luo, and A. T. C. Johnson, *Nano Lett.* **9**, 1472 (2009).
- ⁶R. R. Nair *et al.*, *Appl. Phys. Lett.* **97**, 153102 (2010).
- ⁷X. Li *et al.*, *Science (N.Y.)* **324**, 1312 (2009).
- ⁸Y. Lee, S. Bae, H. Jang, S. Jang, S.-E. Zhu, S. H. Sim, Y. Il Song, B. H. Hong, and J.-H. Ahn, *Nano Lett.* **10**, 490 (2010).
- ⁹X. Li, Y. Zhu, W. Cai, M. Borysiak, B. Han, D. Chen, R. D. Piner, L. Colombo, and R. S. Ruoff, *Nano Lett.* **9**, 4359 (2009).
- ¹⁰J. W. Suk, A. Kitt, C. W. Magnuson, Y. Hao, S. Ahmed, J. An, A. K. Swan, B. B. Goldberg, and R. S. Ruoff, *ACS Nano* **5**, 6916 (2011).
- ¹¹C. R. Dean *et al.*, *Nat. Nanotechnol.* **5**, 722 (2010).
- ¹²Z. H. Ni, H. M. Wang, Z. Q. Luo, Y. Y. Wang, T. Yu, Y. H. Wu, and Z. X. Shen, *J. Raman Spectrosc.* **41**, 479 (2009).
- ¹³J.-H. Chen, C. Jang, S. Adam, M. S. Fuhrer, E. D. Williams, and M. Ishigami, *Nat. Phys.* **4**, 377 (2008).
- ¹⁴A. Nourbakhsh *et al.*, *J. Phys. Chem. C* **114**, 6894 (2010).
- ¹⁵Z. Cheng, Q. Zhou, C. Wang, Q. Li, C. Wang, and Y. Fang, *Nano Lett.* **11**, 767 (2011).
- ¹⁶R. S. Pantelic, J. W. Suk, C. W. Magnuson, J. C. Meyer, P. Wachsmuth, U. Kaiser, R. S. Ruoff, and H. Stahlberg, *J. Struct. Biol.* **174**, 234 (2011).
- ¹⁷R. Zan, U. Bangert, Q. Ramasse, and K. S. Novoselov, *J. Phys. Chem. Lett.* **3**, 953 (2012).
- ¹⁸R. Zan, U. Bangert, Q. Ramasse, and K. S. Novoselov, *Nano Lett.* **11**, 1087 (2011).
- ¹⁹J. Y. Mutus, L. Livadaru, J. T. Robinson, R. Urban, M. H. Salomons, M. Cloutier, and R. A. Wolkow, *New J. Phys.* **13**, 63011 (2011).
- ²⁰H.-W. Fink, W. Stocker, and H. Schmid, *Phys. Rev. Lett.* **65**, 1204 (1990).
- ²¹H. W. Fink, *Recherche* **22**, 964 (1991).
- ²²See: <http://www.acsmaterial.com>.
- ²³S. P. Surwade, Z. Li, and H. Liu, *J. Phys. Chem. C* **116**, 20600 (2012).
- ²⁴See supplementary material at <http://dx.doi.org/10.1116/1.4793746> for movies demonstrating the degradation of PMMA by Pt-metals.
- ²⁵M. M. Hirschler and C. L. Beyler, *SFPE Handbook of Fire Protection Engineering*, 3rd ed. (NFPA, Quincy, 2001).
- ²⁶S. I. Stoliarov, P. R. Westmoreland, M. R. Nyden, and G. P. Forney, *Polymer* **44**, 883 (2003).
- ²⁷M. C. Costache, D. Wang, M. J. Heidecker, E. Manias, and C. A. Wilkie, *Polym. Adv. Technol.* **17**, 272 (2006).
- ²⁸D. Gabor, *Nature* **161**, 777 (1948).
- ²⁹H. W. Fink, *Phys. Scr.* **38**, 260 (1988).
- ³⁰J.-N. Longchamp, T. Latychevskaia, C. Escher, and H.-W. Fink, *Appl. Phys. Lett.* **101**, 113117 (2012).